

Research Article www.acsami.org

High-Ge-Content SiGe Alloy Single Crystals Using the Nanomembrane Platform

Abhishek Bhat, Omar Elleuch,* Xiaorui Cui, Yingxin Guan, Shelley A. Scott, Thomas F. Kuech, and Max G. Lagally



Cite This: ACS Appl. Mater. Interfaces 2020, 12, 20859-20866



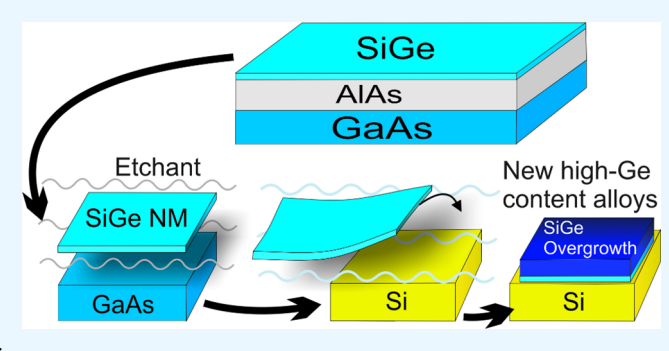
ACCESS

Metrics & More



Supporting Information

ABSTRACT: The growth of single crystals of Ge-rich SiGe alloys in an extended composition range is demonstrated using the nanomembrane (NM) platform and III-V growth substrates. Thin films of high-Ge-content SiGe films are grown on GaAs(001) to below the kinetic critical thickness and released from the growth substrate by selectively etching a release layer to relax the strain. The resulting crystalline nanomembranes at the natural lattice constant of the alloy are transferred to a new host and epitaxially overgrown at similar compositions to make a thicker single crystal. Straightforward critical-thickness calculations demonstrate that a very wide range of group IV alloys, including those involving Sn, can be fabricated using the NM platform and the proper choice of



III-V substrate. Motivations for making new group IV alloys center on band gap engineering for the development of novel group IV optoelectronic structures and devices.

KEYWORDS: SiGe, nanomembrane, overgrowth, III-V, release, transfer

1. INTRODUCTION

There is little debate that silicon, germanium, and their alloys are technologically extremely important. There would be even further applications if thin single-crystal alloys of Si and Ge could be made for a wider range of compositions than is currently possible. Structures containing either strained and/or unstrained SiGe find applications in lasers, high-mobility MOSFETS, quantum computation, and optoelectronics. 1-8 Although Si and Ge are miscible across the complete composition range, the miscibility gap is so large that growing bulk single crystals of alloy at anything but extreme compositions is extremely difficult by conventional bulk growth techniques. Furthermore, the conventional flat geometry in device processing restricts crystal growth approaches to vapor phase epitaxy and is therefore (if single crystals of an alloy are desired9) subject to critical-thickness limitations unless the lattice constant of the substrate can be matched to that of the growing alloy film.

For the conventional Si substrate (and Ge at the opposite end of the composition range), the critical-thickness limitation has in part been circumvented by growing strain-graded buffer layers, in which the composition of each layer changes only slightly, so that the dislocations that form have no or only limited ability to propagate. ^{10–12} An alloy film of the desired composition can be achieved, but with considerable mosaic, surface roughness, and threading dislocations throughout. For

some applications, such a mesoscale morphology is sufficient; 13,14 for many others, it is not. 4,15,16

There is a better way, as we have shown, 17 namely, the application of nanomembrane (NM) technology. In this approach, an alloy film of the desired composition is pseudomorphically grown (i.e., containing strain) to below the critical thickness on the available substrate, released from this host substrate to be free to relax elastically, transferred to a new host, and then overgrown to make an arbitrarily thick strain-free alloy¹⁸ or to grow heterostructures of various designs. 19,20

The essential aspect of this platform is the need for a release layer, so that the desired alloy film can be removed from the rigid substrate on which it is grown. Silicon-on-insulator (SOI) and germanium-on-insulator (GOI) conveniently provide this capability, respectively, for low-Ge-concentration alloys (up to 30% Ge) and low-Si-concentration alloys (~10% Si). Further possibilities for substrates for group IV alloy growth do exist. Specifically, group IV alloys grow epitaxially on group III-V binary and ternary alloys. These substrates not only provide

Received: February 12, 2020 Accepted: April 13, 2020 Published: April 13, 2020







Figure 1. Schematic diagram of growth and release steps for fabricating SiGe NMs. (a) A subcritical-thickness SiGe layer of the desired composition is epitaxially grown on an AlAs release layer initially grown on a GaAs(001) substrate. The arrows indicate tensile strain. (b) The AlAs layer is selectively etched away, causing the release and simultaneous elastic strain relaxation of the SiGe layer. (c) The SiGe NM is transferred to a new host substrate. (d) Any desired lattice-matched or strain-balanced heterostructure or a thicker crystal of the same composition can be grown on the SiGe. The thicknesses of the layers are not drawn to scale. For higher Si concentrations, thin Ge layers are grown below and above the SiGe film to aid in release (see text).

ready release layers for the grown group IV alloy film; they also provide a greater latitude in the group IV alloy compositions that can be achieved, because the lattice constants of the substrate vary directly with its composition, and III—V binary and ternary—alloy growth is well-established.

In this work, we outline the procedures for creating single-crystal Group IV alloy NMs from growth on III–V substrates. We show that these NMs can be transferred to a new host and epitaxially overgrown at similar compositions to make a thicker single crystal. By way of demonstration we fabricate $\mathrm{Si}_x\mathrm{Ge}_{1-x}$ NMs with x varying so far up to 22%, using GaAs(001) as the substrate. We show, via simple critical-thickness calculations, that a very wide range of group IV alloys, including those involving Sn, can be fabricated using the NM platform and the proper choice of substrate.

Apart from a demonstration of the power of the NM platform to create new materials or materials combinations, motivations abound for making new group IV alloys, centering on band gap engineering. For example, the development of Ge inter-subband lasers using the conduction band L valley has been stymied for many years by the lack of good high-Gecontent Si_xGe_{1-x} alloys (0.20 < x < 0.35). These lasers could be realized by creating a heterostructure composed of different alloy compositions of high-Ge-content SiGe layers.^{6,21} Second, as has been demonstrated, 19 the introduction of biaxial tensile strain into the Ge lattice can drive the band structure from indirect to direct, introducing the ability to have a strain controlled wavelength tunable light emitting diode²² or similar devices. Because of the band gap dependence on composition in SiGe alloys, introducing Si modifies the magnitude of the direct gap that will be achievable with biaxial tensile strain. In this context, freestanding and transferable films of these materials are desirable, as they offer a high degree of control over and the ability to manipulate the strain state of the material. Third, replacing Si with Sn to make GeSn alloys can create a direct band gap in a different energy range (0.2 to 0.5 eV depending on strain) and opens the way for novel lowpower and high-mobility group IV electronic and photonic devices. For a cubic lattice, the transition to direct bandgap is assumed to occur around 9% Sn;²³ however, the compressive strain arising from incorporation of the larger-diameter Sn is a critical factor that suppresses the transition to a direct gap,

necessitating even higher Sn concentrations.²⁴ In this respect, the nanomembrane platform is a perfect partner for GeSn and SiGeSn bandgap engineering, facilitating elastic strain relaxation and the opportunity for direct-bandgap GeSn at lower (and more readily achievable) Sn concentrations. The ability to exploit the NM platform should thus expand greatly the sphere of technologies dependent on band structure engineering of group IV materials.

Ge, GaAs, and AlAs are closely lattice matched, with less than 0.15% lattice mismatch between the three materials. Chemical etchants with excellent selectivity are also readily available. The key to the NM platform is to grow a pseudomorphic film below the thickness where it begins to form dislocations, i.e., the kinetic critical thickness.²⁵ given substrate lattice constant, there is always a trade-off between the composition of a growing film and its critical thickness (at a particular growth temperature). So, using an AlAs/GaAs (or In_{0.5}Ga_{0.5}P/GaAs) substrate, we can in principle grow pure Ge to thousands of micrometers, whereas growth of Si_{0.15}Ge_{0.85} is limited to tens of nanometers. Nanomembranes as thin as 20 nm are readily releasable and easily handled. By reducing the substrate lattice constant (e.g., by using a $GaAs_xP_{1-x}$ substrate), either the Si composition in the SiGe can be increased or the critical thickness can be increased (or both to a more limited extent). We have so far grown films with Si concentration as high as x = 22%. By increasing the substrate lattice constant, GeSn films can be grown and GeSn NMs can be fabricated in the same manner.

2. EXPERIMENTAL SECTION

The typical NM fabrication steps, for SiGe NMs grown on III–V substrates, are shown schematically in Figure 1. A release layer of AlAs (200–300 nm) is initially grown on a GaAs(001) substrate (on which generally a GaAs buffer layer is first grown), followed by the subcritical-thickness growth of the intended composition of the SiGe film (Figure 1a). Because of its smaller lattice constant compared to GaAs, the SiGe film is under tensile strain. After removal of the AlAs layer by selective chemical etching (Figure 1b), this strain in the SiGe relaxes elastically. The now free-floating strain-free SiGe NM can be transferred by various means 26,27 to a new host substrate (Figure 1(c)). The transferred SiGe NM acts as the new growth substrate for other SiGe device structures (Figure 1 (d)). Because this NM is elastically relaxed (i.e., at its natural lattice constant), arbitrary

thicknesses of lattice matched device structures or thinner higher-Si-composition alloys (staying below the kinetic critical thickness), can be overgrown. The new NM substrate can also be used for strain balanced heterostructures. We verify the strain state and composition via X-ray diffraction (XRD) and the surface morphologies with atomic force microscopy (AFM). We use cross-sectional scanning electron microscopy (SEM) to view layer thicknesses and uniformity. We also perform Raman spectroscopy to explore to what extent it is useful in providing stain information for these complex structures.

We grew $\mathrm{Si_xGe_{1-x}}/\mathrm{AlAs}$ structures on nominally singular (100) GaAs substrates in a horizontal MOVPE reactor at a pressure of 0.1 bar. Arsine (AsH₃), trimethyl aluminum (Al(CH₃)₃), disilane (0.5% $\mathrm{Si_2H_6}$), and germane (5% GeH₄) were used as the As, Al, Si, and Ge precursors, respectively, with a purified-hydrogen carrier gas at a total flow rate of ~7 slpm (~0.28 mol/min). The growth temperature was 750 °C for AlAs and 565 °C for Ge and $\mathrm{Si_xGe_{1-x}}$. Details of the growth, including a discussion of the physical and chemical factors influencing the growth and thus the uncertainty in the film composition (~1%), are presented elsewhere. After release by selectively etching the AlAs, the SiGe NM is transferred to a Si substrate for subsequent use.

The grown SiGe layer can be released using different methods, depending on the need. In the simplest, useful for small NM sizes, etchant access holes that take up less than a few percent of the area are first lithographically defined on the SiGe film. The film stack is then introduced into a HCl: $\rm H_2O$ 1:7 solution, which selectively etches the AlAs layer and results in a strain-relaxed alloy NM resting on the original GaAs host substrate. After transfer to water, the released SiGe NM floats to the surface, from where it can be transferred to a new host substrate.

The alternative release method uses surface tension to assist in NM release³¹ and negates the need for etchant access holes. This method, which employs a buoyancy layer (e.g., photoresist (PR) or black wax), is appropriate when large-area NMs are desired, and when etchant-access holes are deleterious for a desired application. The Supporting Information describes the release process in detail.

Figure 1 adequately depicts the process for Si compositions up to x=0.15. Alternatively, and certainly for Si concentrations higher than x=15%, we add thin layers of Ge above and below the SiGe film to aid in the release. For growth on AlAs/GaAs, the strain in a Si_15Ge_85 film is \sim 0.58%. The etching is sufficiently aggressive that a thin NM with this magnitude of strain occasionally fractures during release. Making a trilayer sandwich allows strain to be shared between the layers during release, thus (temporarily) reducing the magnitude of the strain relaxation in the alloy NM, and allowing the etch to proceed without fracturing the NM. The Ge layers can be easily removed after release with an appropriate second etching solution, e.g., 3% $\rm H_2O_2$ at 50 °C, at which time the alloy layer completely relaxes; in effect, a two-stage strain relaxation process.

3. RESULTS AND DISCUSSION

3.1. GeSi Film and Nanomembrane Characterization.

To establish that films could be grown continuous and flat, in all cases we performed cross-sectional and plan-view scanning electron microscopy (SEM) on the film stack and the surface of the SiGe film. Figure 2 shows a SEM cross-sectional image of an as-grown nominal $\rm Si_{0.15}Ge_{0.85}/AlAs/GaAs$ structure. The actual composition, determined by XRD, was $\rm Si_{0.14}Ge_{0.86}$.

As mentioned earlier, in order to establish the composition, thickness, crystalline quality, and surface roughness of the SiGe film (still attached) and NM (released, relaxed, and transferred), we used XRD and AFM. Figure 3 shows the XRD scans of a Si_{0.14}Ge_{0.86}(35 nm) layer before and after its release from the growth substrate. XRD determines the layer composition, the strain state before and after release, and the SiGe NM thickness. An XRD scan around the (004) reflection probes the out-of-plane lattice constant and is used to

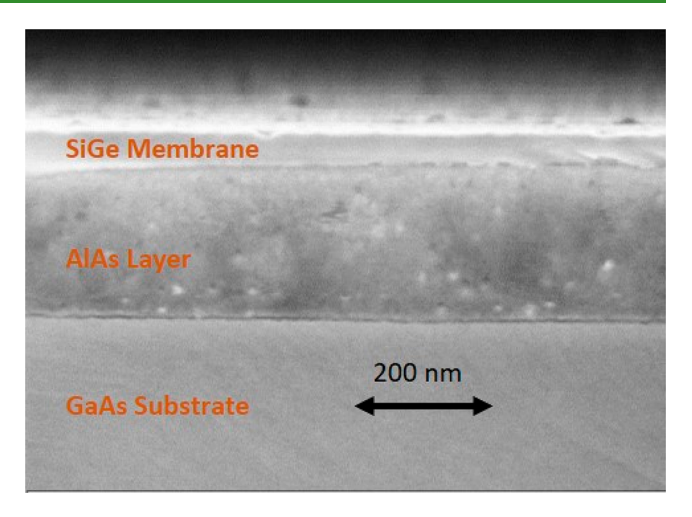


Figure 2. Scanning electron micrograph cross section of a $\rm Si_{0.14}Ge_{0.86}/AlAs/GaAs$ structure, demonstrating the lateral morphology of the pseudomorphic SiGe film. The lattice constant difference between this film and GaAs is 0.03 Å.

determine the composition and thickness of the layers. Figure 3a shows the ω -2 θ (004) scans before and after release along with their corresponding simulated fits. Peaks from larger outof-plane lattice-constant material appear at lower Bragg angle. The SiGe film will be under tensile strain in-plane in the asgrown structure, as it is grown on the larger-lattice-constant AlAs/GaAs substrate. In determining the SiGe composition from the fits, we assume fully strained SiGe (which we show below is true). The thickness and composition determined from the fits are shown in the inset. Overlaid with this scan is the scan after release. Here we only observe a SiGe and Si peak, as the NM was released (AlAs and GaAs removed) and transferred to a new Si host substrate. After release, the SiGe film is no longer pinned at the in-plane lattice constant of its growth substrate, so is free to relax. Consequentially, the inplane strain (which was tensile) relaxes, resulting in an in-plane contraction (and out of plane expansion, as a consequence of Poisson's effect) to the SiGe alloy's bulk lattice constant. This strain relaxation will manifest itself as a peak shift to lower Bragg angle (increasing out-of-plane lattice constant), as shown in Figure 3a. The magnitude of the SiGe peak shift (indicated by the horizontal arrow) corresponds to an elastic strain relaxation of 0.5%, consistent with the predicted magnitude of strain in the as-grown film.

Figure 3b shows a reciprocal-space map of the as-grown structure. A map around the (224) reflection provides information on both in-plane and out-of-plane lattice constants and is used to determine structural coherency and to verify the absence of plastic relaxation. The dashed white line is superimposed as a visual guide to show that the SiGe film and GaAs substrate have the same in-plane lattice constant, i.e., the SiGe film is fully strained to the substrate GaAs lattice. Also, no cross hatch or mosaic, associated with strain-graded growth of alloy compositions at already much lower Si concentrations, is present. These effects are easily observed in reciprocal-space maps as extreme broadening of the intensity. Numerous growths in the range we have attempted, from x = 5 to 22%, show similar XRD results. 30

We use AFM to confirm that release, strain relaxation, and transfer do not significantly affect the surface roughness of the SiGe NM. In all cases, scans were made of different areas on

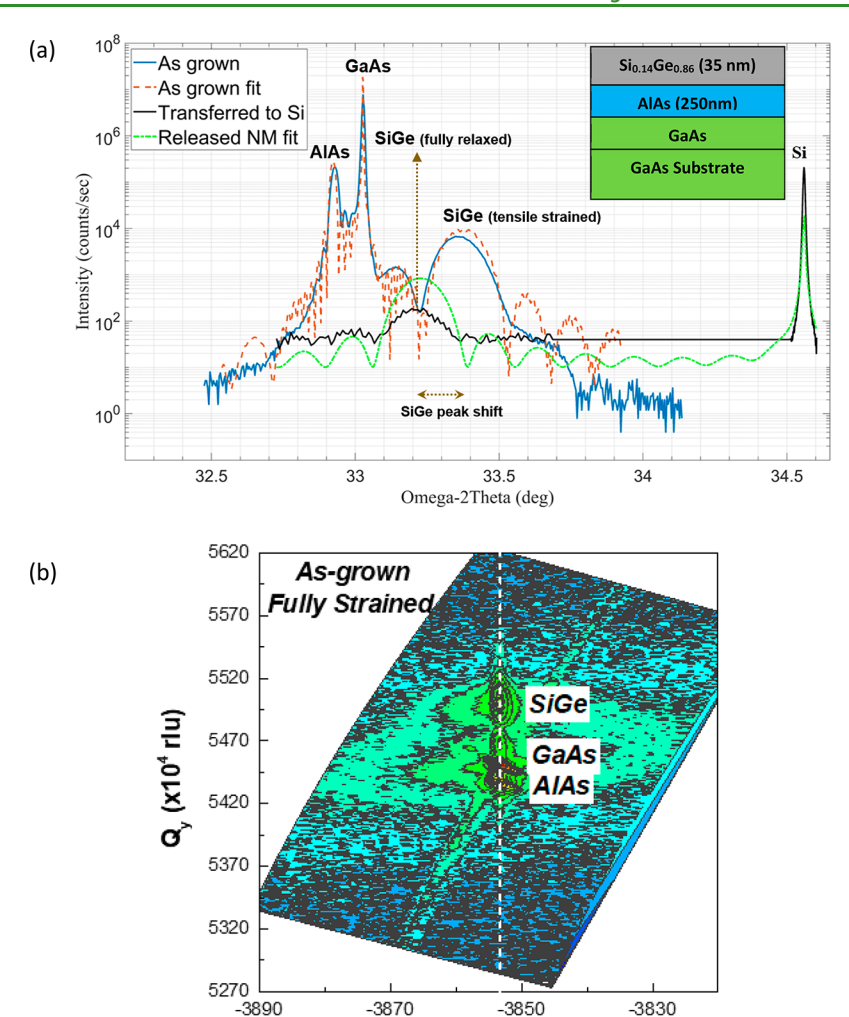


Figure 3. X-ray diffraction data from a 35 nm thick $Si_{0.14}Ge_{0.86}$ NM, confirming the expected NM thickness and composition. (a) $\omega-2\theta$ scan of the as-grown structure in the [004] direction and a similar scan after release and transfer of the NM to a Si host that shows the presence of only the SiGe and Si peaks. Fits to the data are shown by dotted lines. The inset shows the grown heterostructure as confirmed by the XRD spectra. The horizontal arrow shows the shift in the SiGe peak, consistent with the complete elastic relaxation of lattice strain. The line scans for the membrane and the Si substrate were obtained separately and then combined because of variations in the ω angles due to azimuthal-orientation changes during transfer. The strong substrate Si peak also overwhelms the detector and isolating the weak NM signal becomes difficult. Consequently, the region from about 33.6 to 34.4° is not scanned to maintain the signal-to-noise ratio. (b) (224) reciprocal-space map of the as-grown structure showing the SiGe peak in line with the substrate GaAs peak, i.e., fully strained to the GaAs lattice constant. If there were plastic relaxation, the position of the SiGe peak would have shifted to the left. The streak at 30° from the vertical is an instrumental effect.

Q (x10⁴ rlu)

the surface of the film/NM, and in all cases the scan is from the surface that represents the growth front. Experiments on other released NMs have shown little difference in roughness of the two sides. Figure 4 shows a representative scan of the surface of a NM after release and transfer to a Si wafer. AFM measurements of RMS roughness on films and NMs with α varying between 5 and 22% all show similar roughness, with a range from 0.7 to 2.5 nm over a 1 μ m x 1 μ m area. Although these roughnesses are larger than typically found for homoepitaxy, they are in line with other grown and released group IV NMs and in any case sufficiently low so that NMs can serve as new growth substrates.

Raman spectroscopy measurements of the Si–Ge and Ge–Ge lines were also made on these NMs. These are discussed below in conjunction with the same measurements on films overgrown on the NMs. It is important to note here that the Raman spectrometer available for these measurements has a resolution limit of 2 wavenumbers and uses a 532 nm laser,

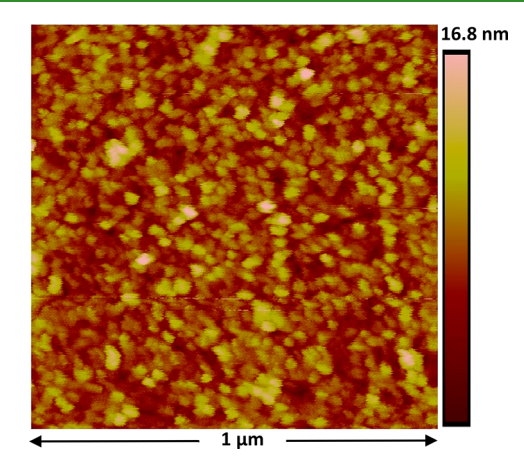


Figure 4. AFM scan of $\mathrm{Si}_{0.14}\mathrm{Ge}_{0.86}$ after release and transfer to an oxidized Si host. The RMS roughness is 2.3 nm.

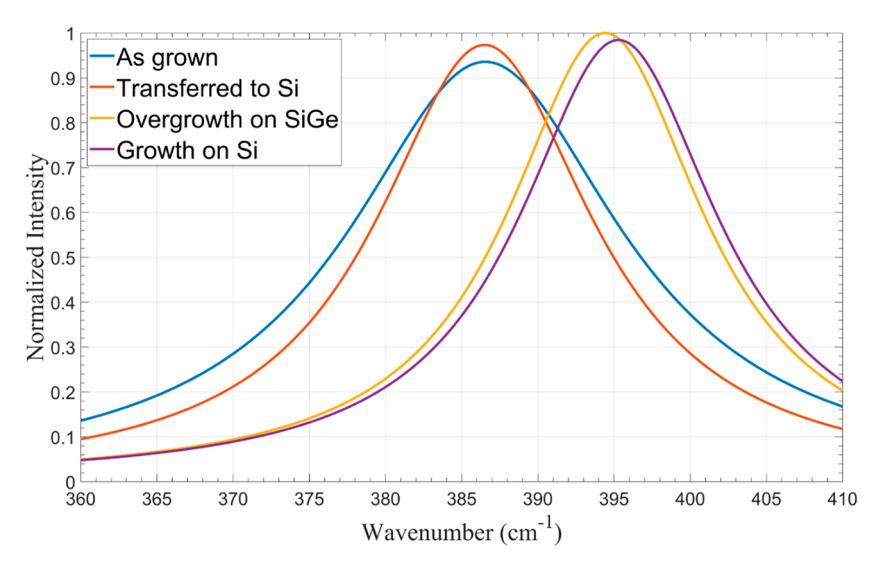


Figure 5. Lorentzian fits to Raman scans of the Si–Ge mode obtained on As-grown $Si_{0.07}Ge_{0.93}$ on GaAs, $Si_{0.07}Ge_{0.93}NM$ released and transferred to Si, 60 nm overgrown $Si_{0.13}Ge_{0.87}$, and the same SiGe grown on the surrounding Si substrate. The blue and red curves are significantly shifted to lower wavenumbers, apparently because of the effect of As doping on the Raman spectrum. The small effect of strain relaxation upon release is not observable in a shift but only a narrowing of the line. $Si_{0.13}Ge_{0.87}$ has a smaller lattice than $Si_{0.07}Ge_{0.93}$. As a result, the overgrown NM has slight tensile strain (\sim 0.25%), as expected from the lattice mismatch. The kinetic critical thickness of $Si_{0.13}Ge_{0.87}$ on Si is less than 10 nm, $^{2.5}$ and as a result, the growth on Si is completely plastically relaxed. This conclusion is validated by the position of the Raman peak.

both less than ideal for the needed measurements, as detailed below. One possibly deleterious consequence of using GaAs as the growth substrate and growing in a III—V MOVPE system is the initial unintentional incorporation of As in the group IV alloy layer. This doping may be detrimental for some electronic applications. However, most of this contamination can be limited to the initial NM layer by proper choice of overgrowth conditions (see below). Doping also influences the position of Raman lines, as discussed below.

3.2. Overgrowth of Thick Films on Transferred NMs.

We now demonstrate our earlier assertion that it is possible to use released and transferred NMs as seed crystals for fabricating thicker homogeneous alloy films. These could be exactly at the same nominal composition as the NM substrate or at a somewhat different composition, as long as we do not exceed the kinetic critical thickness of the film being grown. We describe here the growth of a film with a somewhat higher Si composition, to demonstrate that the process we used initially to grow the NM could be applied also in the overgrowth, to achieve more Si-rich compositions. We grew 60 nm of Si_{0.13}Ge_{0.87} on a 40 nm thick Si_{0.07}Ge_{0.93} NM that was released and transferred to a Si host wafer. The overgrowth was performed in the same MOVPE as the initial NM growth but could as well be carried out with a different method, such as molecular beam epitaxy. The alloy NM and support Si were cleaned (water rinse, HF dip) to remove the oxide from the surfaces of both the NM and the supporting Si before immediate insertion into the growth chamber. The overgrown film covered not only the NM but also the surrounding supporting Si.

Raman spectra for the Si—Ge and Ge—Ge lines, averaged over 100 different locations on the sample, were measured at various stages of the growth, transfer, and overgrowth. ^{32,33} Lorentzian fits to the Si—Ge mode spectra at various stages are presented in Figure 5; original spectra for both lines are shown in the Supporting Information. For the Si_{0.07}Ge_{0.93} NM still attached to the III—V growth substrate, the positions of the Raman peaks suggest an ~1% tensile strain, significantly

greater than the value of 0.25% expected from the lattice mismatch. In addition, the Raman line is broader. The additional shift to lower wavenumbers and the broadening in the Raman peak can be attributed to background As doping during growth. The observed excess shift and the broadening appear to imply a doping level in the low 10¹⁷ range, the limited resolution of the Raman spectrometer, we are not able to distinguish the 0.5 nm shift we expect because of relaxation of the lattice strain for the released NM when the effect of the As doping is also present. However, the Raman line narrows considerably.

Raman traces obtained after transfer of the NM to Si and overgrowth are also shown in Figure 5. The position of the peak after overgrowth of a Si_{0.13}Ge_{0.87} layer on the transferred Si_{0.07}Ge_{0.93} NM indicates an ~0.25% tensile strain, consistent with the strain value of ~0.26% expected between the underlying Si_{0.07}Ge_{0.93} and the Si_{0.13}Ge_{0.87} film. Although no As is deliberately present during the overgrowth, this result alone does not prove that the strain is due to lattice mismatch, as adventitious-As contamination would produce a shift of the Raman line in the same direction. In contrast, the position of the Si–Ge peak for the $Si_{0.13}Ge_{0.87}$ layer grown on the bare Si is at the position expected for completely relaxed Si_{0.13}Ge_{0.87}, consistent with plastic relaxation in this region. The critical thickness of Si_{0.13}Ge_{0.87} grown on Si is maximally several nanometers, so this film must be plastically relaxed. Because there is no change in the Raman peak position from the nostrain value, additionally, the background As doping must be slight or absent in the overgrowth. Any shift to lower wavenumbers seen in the traces due to the presence of As would be evident not just on the overgrowth on the SiGe NM but also on the overgrowth on the Si.

Because the amount of adventitious-As incorporation appears to be negligible, the total amount of As in the sample can be considered as restricted to the initial As that was incorporated in the released NM during the growth of this NM. This As is then buried under the overgrown structure,

thus allaying fears of As incorporation in the final grown structure causing issues in relation to the functionality of electronic devices made from these materials. Bulk diffusion of As can additionally be limited by performing the overgrowth at low temperatures.

3.3. Perspective. *Bilayer Strain Couples*. Just as it has been extensively shown with Si/SiGe strained bilayer strips (strain couples)^{37,38} we can also grow Ge/GeSi films that will curl into tubes, incomplete tubes, or coils, by growing a second layer of a different composition on top of the first, before release.³⁹ Upon release, the differential strain will be shared, resulting in the curling. For example, if released, the above overgrown samples will curl slightly upward to reduce the tensile strain in the top layer by introducing some tensile strain in the bottom layer. These 3D shapes will differ from their counterparts at the other end of the composition range^{36,40,41} herein exhibiting different band structure and different optoelectronic properties.

Other Group IV Alloys and Compositions Based on the NM Platform. Ge NMs. Obviously, pure-Ge NMs can be readily fabricated using growth on GaAs. Ge NMs made in this manner are important, as Ge-on-insulator (GeOI) is no longer commercially available. There are significant potential applications for Ge NMs as growth substrates for graphene sheets and ribbons, 42,43 and for investigations of charge transport in the graphene/Ge system. If externally strained, Ge in NM form can be used as a direct-band gap material in which the band gap may be tunable.

<u>GeSn and SiGeSn</u>. As mentioned in the introduction, GeSn and SiGeSn alloys at various compositions and strains can function as direct-band gap materials for optoelectronic applications, with SiGeSn affording the opportunity to tune the lattice constant and bandgap independently. These films, however, cannot be readily grown at usefully high Sn compositions, in part because of the low miscibility of Sn in Ge but also because of the unavailability of appropriate lattice-matched growth substrates. A possible option to circumvent this problem is to start with growth of a thin NM with the desired composition on a closely lattice matched ternary III–V alloy release layer, such as $In_{0.7}Ga_{0.3}P$ or $In_{0.2}Ga_{0.8}As$ for $Ge_{0.9}Sn_{0.1}$. Figure 6 shows calculations of the kinetic critical

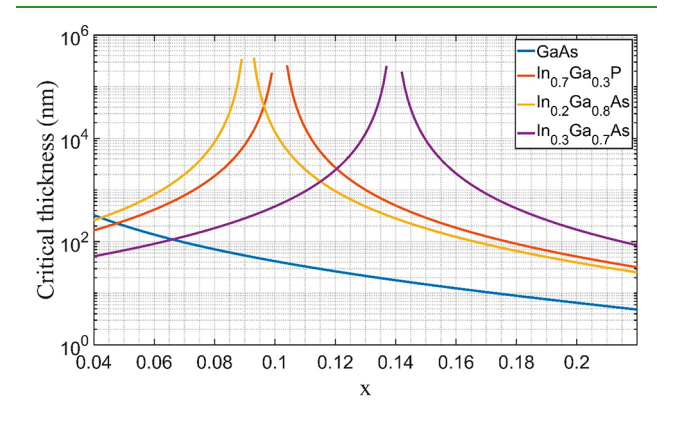


Figure 6. Kinetic critical thickness of $Ge_{1-x}Sn_x$ on InGaP and InGaAs (at two compositions) substrates in the (001 orientation as a function of Sn concentration, X. The curves suggest that more than 40 nm of GeSn can be grown without plastic relaxation on all of these substrates at any Sn concentration from 4 to 20%. The critical thickness of the same GeSn films grown on GaAs (and thus on Ge, as it is closely lattice matched to GaAs) is shown for comparison.

thickness of GeSn on four substrates, as a function of Sn concentration, with the Sn concentration, x, varying up to 22%. Again, selective etchants are available to remove the release layer to create the free-standing GeSn NM, which can then serve as the seed crystal for overgrowth as described above, to make a thick high-Sn-concentration GeSn single crystal. Initial efforts to grow GeSn NMs are in progress. The same procedure will also be applicable for SiGeSn NMs, by adjusting growth substrate lattice constants.

The ability to manipulate the growth substrate lattice constant also allows us to grow slightly tensile-strained GeSn, as we showed for SiGe above. Using tensile strain in the growing NM film will likely aid in the incorporation of Sn, as the lattice will be slightly larger. The NM platform thus makes an interesting test bed for investigating growth kinetics in highly immiscible materials systems, and to explore if a direct-bandgap transition is achievable at a lower Sn concentration via strain management.

4. CONCLUSIONS

We have demonstrated growth of high-Ge-content SiGe NMs on III—V materials, release of these NMs, transfer to new hosts, and overgrowth of similar compositions on these NMs. The crystalline quality of the material is high and is retained after NM transfer to a new host and subsequent overgrowth. Work is underway to grow and release NMs consisting up to 30% Si, as well as on other group IV alloy materials, specifically GeSn, using a range of available III—V alloy growth substrates.

ASSOCIATED CONTENT

Supporting Information

The Supporting Information is available free of charge at https://pubs.acs.org/doi/10.1021/acsami.0c02747.

Description of surface-tension-assisted NM release; Raman characterization depicting the Si–Ge and Ge–Ge modes obtained on as-grown SiGe on GaAs, NM released and transferred to Si, 60 nm overgrown SiGe, and SiGe grown on the surrounding Si substrate (PDF)

AUTHOR INFORMATION

Corresponding Author

Omar Elleuch — Department of Materials Science and Engineering and Department of Chemical and Biological Engineering, University of Wisconsin, Madison, Wisconsin 53706, United States; orcid.org/0000-0003-4908-2062; Email: elleuch@wisc.edu

Authors

Abhishek Bhat — Department of Materials Science and Engineering, University of Wisconsin, Madison, Wisconsin 53706, United States

Xiaorui Cui — Department of Materials Science and Engineering, University of Wisconsin, Madison, Wisconsin 53706, United States

Yingxin Guan — Department of Materials Science and Engineering, University of Wisconsin, Madison, Wisconsin 53706, United States

Shelley A. Scott — Department of Materials Science and Engineering, University of Wisconsin, Madison, Wisconsin 53706, United States; orcid.org/0000-0002-1263-011X

- **Thomas F. Kuech** Department of Chemical and Biological Engineering, University of Wisconsin, Madison, Wisconsin 53706, United States
- Max G. Lagally Department of Materials Science and Engineering, University of Wisconsin, Madison, Wisconsin 53706, United States

Complete contact information is available at: https://pubs.acs.org/10.1021/acsami.0c02747

Notes

The authors declare no competing financial interest.

ACKNOWLEDGMENTS

This research is supported in part by NSF Division of Materials Research through the University of Wisconsin Materials Research Science and Engineering Center (Grants DMR-1121288 and DMR-1720415), and in part by the U.S. Department of Energy, Office of Science, Basic Energy Sciences, Grant DE-FG02-03ER46028. Initial film growth (O.E., Y.G., and T.F.K.) was primarily supported by NSF; NM fabrication and characterization (A.B., X.C., O.E., S.A.S., and M.G.L.) was primarily supported by DOE.

REFERENCES

- (1) Lee, M. L.; Fitzgerald, E. A.; Bulsara, M. T.; Currie, M. T.; Lochtefeld, A. Strained Si, SiGe, and Ge Channels for High-Mobility Metal-Oxide-Semiconductor Field-Effect Transistors. *J. Appl. Phys.* **2005**, *97* (1), 11101.
- (2) Bonfanti, M.; Grilli, E.; Guzzi, M.; Virgilio, M.; Grosso, G.; Chrastina, D.; Isella, G.; von Känel, H.; Neels, A. Optical Transitions in Ge/SiGe Multiple Quantum Wells with Ge-Rich Barriers. *Phys. Rev. B: Condens. Matter Mater. Phys.* **2008**, 78 (4), 41407.
- (3) Schäffler, F. High-Mobility Si and Ge Structures. Semicond. Sci. Technol. 1997, 12 (12), 1515–1549.
- (4) Kuo, Y.-H.; Lee, Y. K.; Ge, Y.; Ren, S.; Roth, J. E.; Kamins, T. I.; Miller, D. A. B.; Harris, J. S. Strong Quantum-Confined Stark Effect in Germanium Quantum-Well Structures on Silicon. *Nature* **2005**, *437* (7063), 1334–1336.
- (5) Tezuka, T.; Sugiyama, N.; Takagi, S. Fabrication of a Strained Is on Sub-10-nm-Thick SiGe-on-Insulator Virtual Substrate. *Mater. Sci. Eng., B* **2002**, *89* (1–3), 360–363.
- (6) Driscoll, K.; Paiella, R. Silicon-Based Injection Lasers Using Electronic Intersubband Transitions in the L Valleys. *Appl. Phys. Lett.* **2006**, *89* (19), 191110.
- (7) Guo, Q.; Di, Z.; Lagally, M. G.; Mei, Y. Strain Engineering and Mechanical Assembly of Silicon/Germanium Nanomembranes. *Mater. Sci. Eng., R* **2018**, *128*, 1–31.
- (8) Huang, M.; Cavallo, F.; Liu, F.; Lagally, M. G. Nanomechanical Architecture of Semiconductor Nanomembranes. *Nanoscale* **2011**, 3 (1), 96–120.
- (9) Matthews, J. W.; Blakeslee, A. E. Defects in Epitaxial Multilayers. *J. Cryst. Growth* **1976**, 32 (2), 265–273.
- (10) Shah, V. A.; Dobbie, A.; Myronov, M.; Fulgoni, D. J. F.; Nash, L. J.; Leadley, D. R. Reverse Graded Relaxed Buffers for High Ge Content SiGe Virtual Substrates. *Appl. Phys. Lett.* **2008**, 93 (19), 192103.
- (11) Venkatasubramanian, R.; Timmons, M. L.; Mantini, M.; Kao, C. T.; Parikh, N. R. Heteroepitaxy and Characterization of Gerich SiGe Alloys on GaAs. *J. Appl. Phys.* **1991**, *69* (12), 8164–8167.
- (12) Rim, K.; Hoyt, J. L.; Gibbons, J. F. Fabrication and Analysis of Deep Submicron Strained-Si n-MOSFET's. *IEEE Trans. Electron Devices* **2000**, *47* (7), 1406–1415.
- (13) Fitzgerald, E. A.; Xie, Y.-H.; Monroe, D.; Silverman, P. J.; Kuo, J. M.; Kortan, A. R.; Thiel, F. A.; Weir, B. E. Relaxed Ge_xSi_{1-x} Structures for III–V Integration with Si and High Mobility Two-

- Dimensional Electron Gases in Si. J. Vac. Sci. Technol., B: Microelectron. Process. Phenom. 1992, 10 (4), 1807.
- (14) Gallas, B.; Hartmann, J. M.; Berbezier, I.; Abdallah, M.; Zhang, J.; Harris, J. J.; Joyce, B. A. Influence of Misfit and Threading Dislocations on the Surface Morphology of SiGe Graded-Layers. *J. Cryst. Growth* **1999**, 201–202, 547–550.
- (15) Sakai, A.; Taoka, N.; Nakatsuka, O.; Zaima, S.; Yasuda, Y. Substrate for Epitaxial Growth, Process for Producing the Same, and Multi-Layered Film Structure U.S. Patent 2006, 0011916A1.
- (16) Sakai, A.; Taoka, N.; Nakatsuka, O.; Zaima, S.; Yasuda, Y. Pure-Edge Dislocation Network for Strain-Relaxed SiGe/Si(001) Systems. *Appl. Phys. Lett.* **2005**, *86* (22), 221916.
- (17) Roberts, M. M.; Klein, L. J.; Savage, D. E.; Slinker, K. A.; Friesen, M.; Celler, G.; Eriksson, M. A.; Lagally, M. G. Elastically Relaxed Free-Standing Strained-Silicon Nanomembranes. *Nat. Mater.* **2006**, *5* (5), 388–393.
- (18) Paskiewicz, D. M.; Savage, D. E.; Holt, M. V.; Evans, P. G.; Lagally, M. G. Nanomembrane-Based Materials for Group IV Semiconductor Quantum Electronics. Sci. Rep. 2015, 4, 4218.
- (19) Sookchoo, P.; Sudradjat, F. F.; Kiefer, A. M.; Durmaz, H.; Paiella, R.; Lagally, M. G. Strain Engineered SiGe Multiple-Quantum-Well Nanomembranes for Far-Infrared Intersubband Device Applications. *ACS Nano* **2013**, *7* (3), 2326–2334.
- (20) Knapp, T. J.; Mohr, R. T.; Li, Y. S.; Thorgrimsson, B.; Foote, R. H.; Wu, X.; Ward, D. R.; Savage, D. E.; Lagally, M. G.; Friesen, M.; Coppersmith, S. N.; Eriksson, M. A. Characterization of a Gate-Defined Double Quantum Dot in a Si/SiGe Nanomembrane. *Nanotechnology* **2016**, *27* (15), 154002.
- (21) Driscoll, K.; Paiella, R. Design of N-Type Silicon-Based Quantum Cascade Lasers for Terahertz Light Emission. *J. Appl. Phys.* **2007**, *102* (9), 093103.
- (22) Sänchez-Pérez, J. R.; Lagally, M. G. Strain Tunable Light Emitting Diodes with Germanium P-I-N Heterojunctions. U.S. Patent 2015, 0129911A1.
- (23) Wirths, S.; Geiger, R.; von den Driesch, N.; Mussler, G.; Stoica, T.; Mantl, S.; Ikonic, Z.; Luysberg, M.; Chiussi, S.; Hartmann, J. M.; Sigg, H.; Faist, J.; Buca, D.; Grützmacher, D. Lasing in Direct-Bandgap GeSn Alloy Grown on Si. *Nat. Photonics* **2015**, 9 (2), 88–92.
- (24) Wirths, S.; Buca, D.; Mantl, S. Si-Ge-Sn Alloys: From Growth to Applications. *Prog. Cryst. Growth Charact. Mater.* **2016**, 62 (1), 1–39
- (25) People, R.; Bean, J. C. Calculation of Critical Layer Thickness versus Lattice Mismatch for Ge_xSi_{1-x}/Si Strained-Layer Heterostructures. *Appl. Phys. Lett.* **1985**, 47 (3), 322.
- (26) Scott, S. A.; Lagally, M. G. Elastically Strain-Sharing Nanomembranes: Flexible and Transferable Strained Silicon and Silicon–Germanium Alloys. *J. Phys. D: Appl. Phys.* **2007**, *40* (4), R75–R92.
- (27) Carlson, A.; Bowen, A. M.; Huang, Y.; Nuzzo, R. G.; Rogers, J. A. Transfer Printing Techniques for Materials Assembly and Micro/Nanodevice Fabrication. *Adv. Mater.* **2012**, 24 (39), 5284–5318.
- (28) Elleuch, O.; Lekhal, K.; Guan, Y.; Kuech, T. F. Highly Tin Doped GaAs at Low Growth Temperatures Using Tetraethyl Tin by Metal Organic Vapor Phase Epitaxy. *J. Cryst. Growth* **2019**, *507*, 255–259.
- (29) Zhang, Z.; Lagally, M. G. Atomistic Processes in the Early Stages of Thin-Film Growth. *Science* **1997**, *276*, *377*–388.
- (30) Elleuch, O.; Bhat, A.; Cui, X.; Guan, Y.; Lekhal, K.; Scott, S.A.; Lagally, M.G.; Kuech, T.F. Growth of High-Ge-Composition Ge/ Si_xGe_{1-x}/Ge Trilayers using Metalorganic Vapor Phase Epitaxy, in progress.
- (31) Cheng, C.-W.; Shiu, K.-T.; Li, N.; Han, S.-J.; Shi, L.; Sadana, D. K. Epitaxial Lift-off Process for Gallium Arsenide Substrate Reuse and Flexible Electronics. *Nat. Commun.* **2013**, *4*, 1577.
- (32) Pezzoli, F.; Martinelli, L.; Grilli, E.; Guzzi, M.; Sanguinetti, S.; Bollani, M.; Chrastina, H. D.; Isella, G.; Känel, H. von; Wintersberger, E.; Stangl, J.; Bauer, G. Raman Spectroscopy of Si_{1-x}Ge_x Epilayers. *Mater. Sci. Eng., B* **2005**, 124–125 (SUPPL), 127–131.

- (33) Pezzoli, F.; Bonera, E.; Grilli, E.; Guzzi, M.; Sanguinetti, S.; Chrastina, D.; Isella, G.; von Känel, H.; Wintersberger, E.; Stangl, J.; Bauer, G. Phonon Strain Shift Coefficients in Si_{1-x}Ge_x Alloys. *J. Appl. Phys.* **2008**, *103* (9), 093521.
- (34) Doehler, J. Raman Scattering from Electronic Excitations in Ge. *Phys. Rev. B* **1975**, *12* (8), 2917–2931.
- (35) Doehler, J.; Colwell, P. J.; Solin, S. A. Raman Scattering from Semiconducting and Metallic Ge(As). *Phys. Rev. Lett.* **1975**, 34 (10), 584–587.
- (36) Cerdeira, F.; Cardona, M. Effect of Carrier Concentration on the Raman Frequencies of Si and Ge. *Phys. Rev. B* **1972**, *5* (4), 1440–1454.
- (37) Qin, H.; Shaji, N.; Merrill, N. E.; Kim, H. S.; Toonen, R. C.; Blick, R. H.; Roberts, M. M.; Savage, D. E.; Lagally, M. G.; Celler, G. Formation of Microtubes from Strained SiGe/Si Heterostructures. *New J. Phys.* **2005**, *7* (05), 241.
- (38) Jin-Phillipp, N. Y.; Thomas, J.; Kelsch, M.; Deneke, C.; Songmuang, R.; Schmidt, O. G. Electron Microscopy Study on Structure of Rolled-up Semiconductor Nanotubes. *Appl. Phys. Lett.* **2006**, *88* (3), 033113.
- (39) Yu, M.; Huang, Y.; Ballweg, J.; Shin, H.; Huang, M.; Savage, D. E.; Lagally, M. G.; Dent, E. W.; Blick, R. H.; Williams, J. C. Semiconductor Nanomembrane Tubes: Three-Dimensional Confinement for Controlled Neurite Outgrowth. *ACS Nano* **2011**, *5* (4), 2447–2457.
- (40) Huang, M.; Boone, C.; Roberts, M.; Savage, D. E.; Lagally, M. G.; Shaji, N.; Qin, H.; Blick, R.; Nairn, J. A.; Liu, F. Nanomechanical Architecture of Strained Bilayer Thin Films: From Design Principles to Experimental Fabrication. *Adv. Mater.* **2005**, *17* (23), 2860–2864.
- (41) Cavallo, F.; Lagally, M. G. Nano-Origami: Art and Function. *Nano Today* **2015**, *10* (5), 538–541.
- (42) Wang, G.; Zhang, M.; Zhu, Y.; Ding, G.; Jiang, D.; Guo, Q.; Liu, S.; Xie, X.; Chu, P. K.; Di, Z.; Wang, X. Direct Growth of Graphene Film on Germanium Substrate. Sci. Rep. 2013, 3 (1), 2465.
- (43) Jacobberger, R. M.; Kiraly, B.; Fortin-Deschenes, M.; Levesque, P. L.; McElhinny, K. M.; Brady, G. J.; Rojas Delgado, R.; Singha Roy, S.; Mannix, A.; Lagally, M. G.; Evans, P. G.; Desjardins, P.; Martel, R.; Hersam, M. C.; Guisinger, N. P.; Arnold, M. S. Direct Oriented Growth of Armchair Graphene Nanoribbons on Germanium. *Nat. Commun.* **2015**, *6* (1), 8006.
- (44) Rojas Delgado, R.; Jacobberger, R. M.; Roy, S. S.; Mangu, V. S.; Arnold, M. S.; Cavallo, F.; Lagally, M. G. Passivation of Germanium by Graphene. *ACS Appl. Mater. Interfaces* **2017**, 9 (20), 17629–17636.
- (45) Sänchez-Pérez, J. R.; Boztug, C.; Chen, F.; Sudradjat, F. F.; Paskiewicz, D. M.; Jacobson, R.; Lagally, M. G.; Paiella, R. Direct-Bandgap Light-Emitting Germanium in Tensilely Strained Nanomembranes. *Proc. Natl. Acad. Sci. U. S. A.* **2011**, *108* (47), 18893–18898
- (46) Boztug, C.; Sánchez-Pérez, J. R.; Cavallo, F.; Lagally, M. G.; Paiella, R. Strained-Germanium Nanostructures for Infrared Photonics. ACS Nano 2014, 8 (4), 3136–3151.